Phase stability of the rare-earth sesquioxides under pressure

M. Rahm and N. V. Skorodumova
Division of Materials Theory, Department of Physics and Material Science, Uppsala University, P.O. Box 530, SE-75121 Uppsala, Sweden

(Received 27 February 2009; revised manuscript received 17 August 2009; published 16 September 2009)

The relative phase stability of the C- and A-type polymorphs of rare-earth sesquioxides RE_2O_3 (RE=La, Ce, Pr, Nd, Pm, Sm, Gd, Er, and Lu) under pressure have been studied by *ab initio* methods based on density-functional theory within the local-density approximation (LDA), and generalized gradient approximation. Both functionals show that the pressure of the C- to A-phase transition increases in the oxide series, although, the LDA results appear to be in better agreement with experimental data. The equation of states and pressure dependence of bulk modulus, c/a ratio and other structural parameters are analyzed. Our results indicate that the phase stability in these oxides to a large extend is determined by the electrostatic contribution to the total energy and it is related to the relaxation pattern of the structures.

DOI: 10.1103/PhysRevB.80.104105 PACS number(s): 71.20.Eh, 71.15.Mb

I. INTRODUCTION

Rare-earth (RE_2O_3) sesquioxides are important materials for different technological applications requiring specific catalytic, magnetic, and electronic properties.[1–3] This makes it crucial to understand the relation among polymorphic forms of these materials at different conditions. Below 2000 °C RE_2O_3 are known to exist in three polymorphic forms: hexagonal A type ($P\bar{3}m1$), monoclinic B type ($C2/m$), and cubic C type ($Ia\bar{3}$),[4] and above this temperature the appearance of X and H phases has been reported.[5] Lighter RE_2O_3 adopt the A-type structure, heavier RE_2O_3 prefer the C type whereas the middle oxides (Sm to Gd) can be stabilized in C and B types depending on temperature.[6] Pressure is expected to promote the stability of A type over C type as the molar volume is found to decrease in the phase sequence C-B-A.[7] Previous experimental studies confirm the stabilization of denser B phase by pressure and indicate that it could be metastable even at ambient conditions.[7]

Earlier studies have revealed many important details of the electronic, optical, and structural properties of RE_2O_3.[8–13] The unit cell of the cubic C-type structure can be built out of 8 unit cell of fluorite structure ($Fm3m$) by removing 25% of oxygen atoms and ordering the remaining oxygens in a specific way[9] [Fig. 1(a)]. In such a structure each RE atom has six oxygens and two vacancies in its first coordination shell arranged in two distinct ways: one type of RE (RE1) has oxygen vacancies aligned along the (111) direction [Fig. 1(b)] and the other one (RE2) has them along (110) [Fig. 1(b)]. Each oxygen atom in the C-type Re_2O_3 is surrounded by four RE atoms and in the ideal structure it is situated in the middle of RE tetrahedron [Fig. 1(b)]. In real structures atoms are slightly shifted from the ideal positions shown in Fig. 1. The unit cell of the hexagonal A-type structure contains two RE and three oxygen atoms [Fig. 1(c)]. Both RE atoms are situated in distorted tetrahedrons formed by four oxygens being equivalent with respect to their oxygen coordination. At the same time we find two types of oxygen atoms with respect to their RE coordination: two out of three oxygens (O1) are found in the tetrahedron of four RE atoms but the third oxygen (O2) is surrounded by six RE atoms situated at relatively large distances [Fig. 1(c)].

The stoichiometry of sesquioxides (RE_2O_3) implies the 3+ valence state of the rare-earth elements in these oxides that appears to be confirmed experimentally.[14,15] RE_2O_3 oxides are insulating materials where each rare-earth atom donates three electrons to fill the p band of oxygen dominating the oxide valence band. Theoretical modeling of rare-earth compounds is a challenging task due to the presence of partially filled 4f states which are poorly described by conventional density-functional schemes drastically underestimating the on-site Coloumb repulsion of f electrons. However, it has been demonstrated for Ce_2O_3 that Ce 3+ can be modeled within the core state model (CSM) treating the 4f orbital as core states.[8] Moreover, CSM has successfully been applied to study the properties of ceria doped with various RE elements.[8] Using this approach Hirosaki *et al.*[16] have described the structural properties of most of A- and C-type RE_2O_3.[12] These studies have demonstrated that the core state model gives satisfactory results when one needs to compare different structures of Re_2O_3.[8,12,16] However, if one wants to study different oxidation states of RE atoms corresponding to

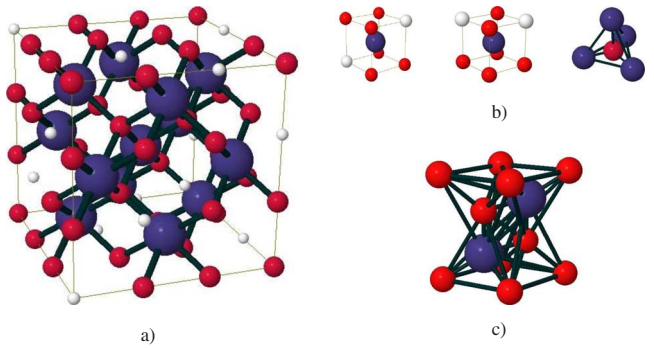

FIG. 1. (Color online) The unit cells of (a) cubic C-type and (c) hexagonal A-type RE_2O_3.(b) In the ideal cubic structure oxygen atoms are situated in the center of tetrahedrons formed by RE atoms, the RE atoms are surrounded by six oxygens arranged in two different ways corresponding to the vacancy alignment along the (111) and (110) directions (b). The RE atoms are shown in blue (dark gray), oxygens are in red (light gray), vacancy positions are indicated by white spheres.

different localization states of $4f$ electrons one should apply more sophisticated approaches. In particular, the LDA+U approach has been shown to give a good description of both CeO_2 and Ce_2O_3 as well as the oxygen vacancy formation energy.[10,17] Using the self-interaction-corrected (SIC) local-spin-density approach Petit *et al.*[11] have demonstrated that RE sesquioxides prefer trivalent electronic configuration. The transition from sesquioxides to dioxides is found to be accompanied by f-electron localization.[9,11]

Here we apply the core state model to study the properties of the A- and C-type structures of the RE sesquioxides (*RE* =La, Ce, Pr, Nd, Pm, Sm, Gd, Er, and Lu) and their relative stability under pressure. Generally the understanding of the property changes induced by compression is of a wide fundamental interest. Moreover, computational techniques also allow us to study materials under extension, that is, difficult to do in experiment. The information about the property trends in RE oxide series can be important for applications relying on the characteristics of mixed rare-earth oxides[2] as well as for the development of novel complex heterogeneous structures. The pressure of the C- to A-phase transition is obtained based on the comparison of the enthalpies of the two phases and mechanisms driving this transition are discussed. The rest of the paper is organized as follows. In Sec. II we give the computational details. Sec III is devoted to the discussion of the obtained equilibrium and high-pressure properties, trends in the oxide series, structural relaxation patterns, and phase transition. Concluding remarks can be found in Sec. IV.

II. DETAILS OF CALCULATIONS

The calculations were done using the projector-augmented wave method (PAW) (Refs. 18 and 19) [as implemented in VASP (Ref. 20)] in the framework of density-functional theory (DFT). The exchange-correlation effects were treated using both the local-density approximation (LDA) and generalized gradient approximation (GGA) in the Perdew-Burke-Ernzerhof[21] parametrization. In all the cases the f orbitals of RE atoms were treated in CSM as a part of inert core, which in practice means the usage of the PAW potentials generated for this particular orbital configuration. Integration over the Brillouin-zone (BZ) was performed using $13\times13\times13$ Monkhorst-Pack[22] grid for the A type and the $6\times6\times6$ grid for the cubic C-type cell. The cutoff energy in the calculations was 500 eV. These parameters ensured the convergence of the total energies within 1 meV/atom.

The ion positions and cell shapes of all the calculated structures were optimized at each volume. The relaxation cycle was stopped when the Hellman-Feynman forces were smaller than 10^{-2} eV/Å. During the relaxation the BZ integration was done using Gaussian smearing with 0.2 eV. The total energies of the relaxed structures were then recalculated using the tetrahedron method with Blöchl corrections[23] for the BZ integration. For each compound and structure the total energies were calculated for a set of volumes around the equilibrium volume thus obtaining the energy versus volume $[E(V)]$ dependence for each case. The $E(V)$ data was fitted to the Birch-Murnaghan equation of states[24] and the equilibrium volume, bulk modulus and enthalpy as functions of pressure $[H(P)]$ were extracted. The $H(P)$ curves were then used to determine the stability regions of the A- and C-type structures and transition pressure.

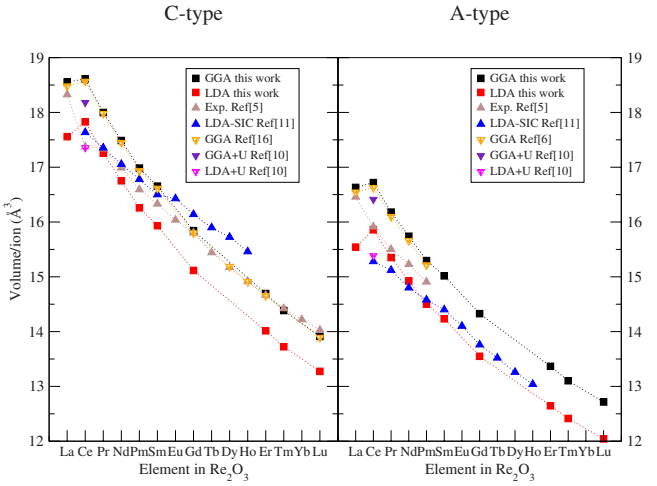

FIG. 2. (Color online) Equilibrium volumes for (a) C-type and (b) A-type RE_2O_3 calculated using both GGA and LDA in comparison with available experimental and theoretical data.

III. RESULTS AND DISCUSSION

A. Equilibrium properties

The calculated equilibrium volumes per formula unit demonstrate a fair agreement with both experimental data and previous calculations[5,8,11,16] (Fig. 2). Generally GGA tends to overestimate equilibrium volumes whereas LDA underestimates them. In the case of the A-type structures the equilibrium volumes calculated using the GGA are larger than the experimentally obtained values[5] (Fig. 2). For the C type we observe the same trend except for the oxides of heaviest RE where our calculations give almost experimental or even slightly lower values [Fig. 1(a)]. The LDA volumes are systematically lower than the experimentally measured ones, except for Ce_2O_3 for which LDA gives relatively high equilibrium volume [Fig. 1(b)]. The comparison of our results to those obtained by the SIC method[11] reveals a somewhat better agreement in the case the A-type phase compared to C type. We notice, however, that the LDA-SIC calculations were performed without any relaxation of internal atomic positions and for the experimental c/a ratios of the A-type structures.[11]

The equilibrium volumes of both phases decrease from Ce to Lu that is in agreement with the ion contraction observed throughout the lanthanide series. The equilibrium volume of the A-type structure is regularly smaller than that of C type for all the oxides. Our calculations result in a smaller volume for La_2O_3 compared to Ce_2O_3 that, though in agreement with previous calculations,[16] seems to be at variance with the experimental data by Adachi *et al.*[5] For both A- and C-type structures Adachi *et al.*[5] report a smaller volume for Ce_2O_3 as compared to La_2O_3 and in the case of C-type Ce_2O_3 it is also smaller than the volume of Nd_2O_3. We notice, however,

TABLE I. Equilibrium volumes, c/a ratios and bulk moduli of A- and C-type RE_2O_3 calculated within the CSM approach.

	A type						C type			
	V (Å^3/atom)		c/a		B (GPa)		V (Å^3/atom)		B (GPa)	
Oxide	GGA	LDA	GGA	LDA	GGA	LDA	GGA	LDA	GGA	LDA
La_2O_3	16.63	15.54	1.573	1.535	109.3	123.8	15.56	17.56	113.1	123.5
Ce_2O_3	16.72	15.86	1.575	1.543	112.0	125.9	18.61	17.83	113.3	129.9
Pr_2O_3	16.18	15.35	1.573	1.544	114.5	130.8	18.00	17.26	118.2	134.3
Nd_2O_3	15.74	14.93	1.576	1.547	120.5	136.7	17.49	16.75	122.8	139.2
Pm_2O_3	15.30	14.50	1.579	1.548	124.2	141.1	16.98	16.26	126.2	144.3
Sm_2O_3	15.02	14.23	1.582	1.553	126.4	144.3	16.66	15.93	127.7	146.7
Gd_2O_3	14.33	13.55	1.590	1.563	132.7	152.4	15.84	15.12	135.2	154.9
Er_2O_3	13.37	12.65	1.601	1.574	143.1	164.1	14.69	14.01	146.0	167.5
Tm_2O_3	13.10	12.41	1.606	1.577	145.6	168.8	14.38	13.72	149.0	171.2
Lu_2O_3	12.72	12.04	1.616	1.588	152.0	174.9	13.91	13.27	152.2	175.3

the experiments for Ce_2O_3 were done on substoichiometric samples $Ce_2O_{1.53-1.50}$. The presence of smaller Ce^{4+} ions decreases the lattice volume that could be the reason for the discrepancy between the theory and experiment.

The calculated equilibrium volumes, c/a ratios for the A-type structure and bulk moduli, extracted from the fit to the Birch-Murnaghan equation of states, are summarized in Table I. The c/a ratio and bulk modulus increase from La to Lu. This correlates well with the volume decrease and corresponding density increase throughout the series that should lead to an increasing stiffness from La to Lu. Despite of a smaller equilibrium volume/atom the A-type structure appears to be slightly softer than C type for all considered RE_2O_3 (Table I).

B. High-pressure properties and phase transition

Relative stability of the A- and C-type structures under pressure was studied by comparing the enthalpies of the phases. The phase diagram obtained using LDA and GGA is shown in Fig. 3. Although the LDA transition pressures are systematically lower than the GGA ones by about 4–5 GPa both functionals demonstrate the same trend with the transition pressure increasing with increasing RE atomic number. This 4–5 GPa shift, however, leads to a qualitatively different result. At ambient pressure GGA predicts all sesquioxides to be stable in the C-type structure that contradicts the experimental observations. LDA, on the other hand, to a good extent reproduces the reported experimental behavior with A-type favored at ambient pressure for oxides up to Sm_2O_3 and C-type stable for heavier Re_2O_3. Similar discrepancy between the LDA and GGA results has previously been reported by Da Silva[10] for Ce_2O_3. His calculations were done using both LDA(GGA) and LDA(GGA)+U approaches (Ce 4f states in the valence band) applying the PAW potentials (VASP) as well as the full potential LAPW method.[10] Regardless of what DFT method was used GGA always predicted higher stability of the C phase that implies that for Ce this behavior is neither due to the localization of the f electrons nor relativistic effects. Therefore, the overestimation of the cubic structure stability seems to be a feature of GGA whereas LDA appears to provide a better agreement with experimental data. We notice that our approach is based on the comparison of the enthalpies of the two phases and provides no estimation of the possible energy barrier or activation energy of the transition. Therefore, it gives us a minimal estimate of the transition pressure not taking into account kinetic effects.

The comparison of the calculated equations of states (EOS) shows that the volume change across the transition is quite substantial. To avoid overloaded pictures we illustrate this by showing EOS for La_2O_3, Pr_2O_3, Sm_2O_3, and Tm_2O_3 calculated using LDA (Fig. 4). For La_2O_3 the volume change is about 11.2% (LDA) and it is gradually decreases throughout the series down to 9.19% (LDA) for Lu_2O_3. The corresponding values obtained in the GGA calculations are lower by about 0.4% (not shown). The slopes of the EOS curves steepen from La to Lu indicating the increasing stiffness of

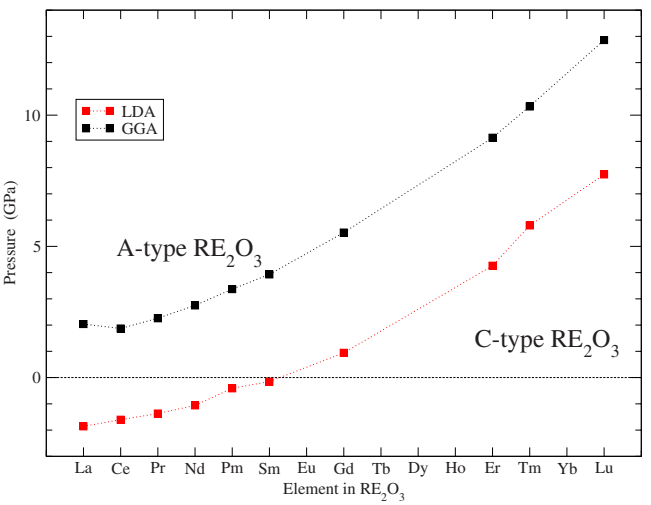

FIG. 3. (Color online) Transition pressures for the C- to A-phase transition calculated for RE_2O_3 using LDA and GGA.

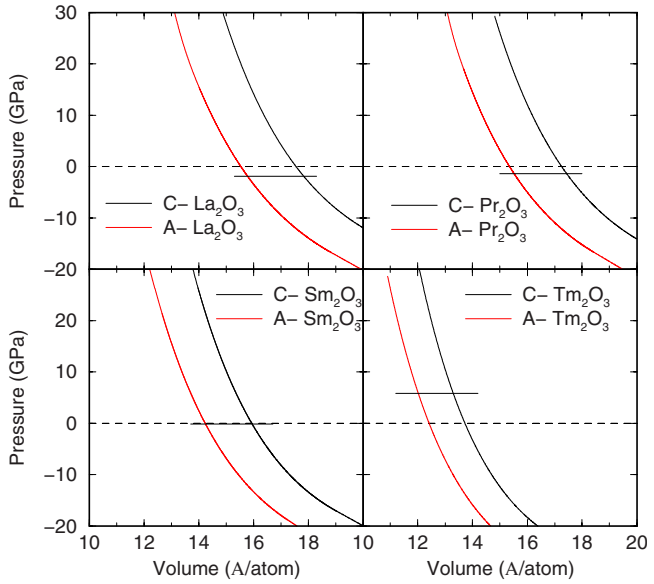

FIG. 4. (Color online) The equation of states for the C- and A-type structures of La_2O_3, Pr_2O_3, Sm_2O_3, and Tm_2O_3 obtained using the LDA approximation. For each case zero pressure is indicated by the dashed line, solid line shows the C- to A-transition pressure.

the oxides in the series. The trend is confirmed by the calculated pressure dependence of bulk moduli (Fig. 5). Bulk moduli increase under pressure for all the oxides, although this increase is steeper for the cubic oxides than for the corresponding hexagonal phases. More detailed comparison reveals that the gradient of the pressure dependence of the bulk modulus does not differ especially much for different cubic Re_2O_3, whereas in the case of the hexagonal phase we observe a more noticeable rate of bulk modulus increase for heavier Re_2O_3 than for the lighter ones. We illustrate this observation by showing dB/dP for Pr_2O_3 and Tm_2O_3 phases (Fig. 5, insert).

These substantial changes in the behavior of A type Re_2O_3 are determined by the adjustments of the hexagonal structure

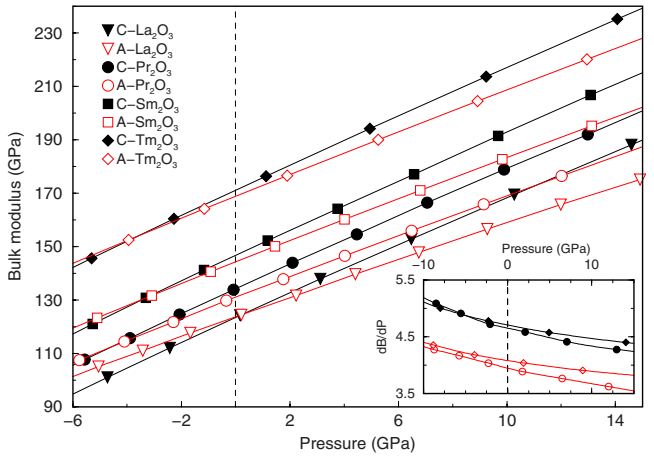

FIG. 5. (Color online) The pressure dependence of bulk moduli of the C- and A-type structures of La_2O_3, Pr_2O_3, Sm_2O_3, and Tm_2O_3 obtained using the LDA approximation. The pressure dependences of dB/dP for Pr_2O_3 and Tm_2O_3 are shown in the insert.

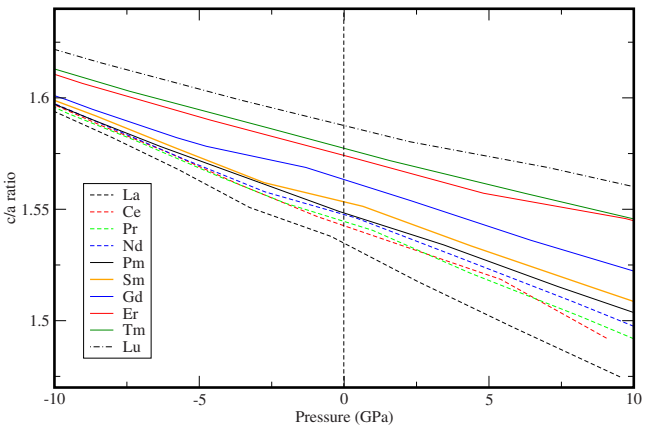

FIG. 6. (Color online) The pressure dependence of the c/a ratio of hexagonal RE_2O_3 obtained using the LDA approximation.

under pressure. The c/a ratios of all the hexagonal oxides decrease under pressure but this decrease is more pronounced for lighter RE than for heavier ones (Fig. 6). Figure 6 demonstrates that the c/a ratios of all the A-type oxides become closer to each other at expansion and increasingly deviate from each other under compression. Larger c/a ratios and smaller volumes of heavier A type Re_2O_3 mean that the tetrahedrons of oxygen and RE atoms are more distorted in heavier Re_2O_3 compared to lighter oxides. Figure 7 shows the oxygen-RE distances in A-type Pr_2O_3 and Tm_2O_3 as the functions of atomic volume. In the A-type structure there are two types of oxygen atoms, O1 situated in the tetrahedrons of RE atoms and O2 surrounded by six RE [Fig. 1(c)]. The tetrahedrons are not perfect and they are characterized by

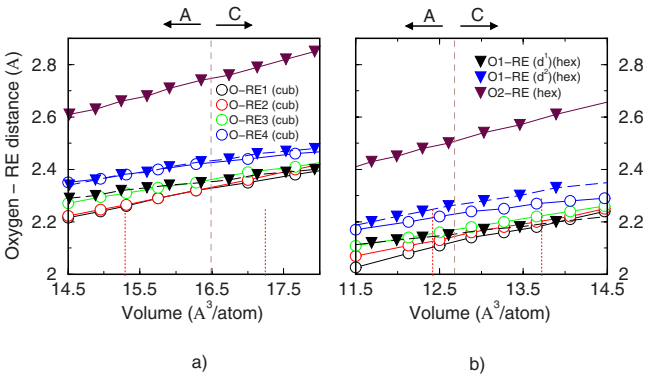

FIG. 7. (Color online) The volume dependence of oxygen—RE distances obtained for the C and A phase of (a) Pr_2O_3 and (b) Tm_2O_3 using LDA. In the ideal cubic structure oxygen is situated in the middle of RE tetrahedron [Fig. 1(b)], therefore, there is only one O-RE distance. In real structures the tetrahedron is distorted and O-RE distances vary. The distances between oxygen and each of the four RE atoms constituting the RE tetrahedrons are shown by empty circles. In the hexagonal structure [Fig. 1(c)] the tetrahedrons are not perfect either and they are characterized by two distances, a shorter one (d^1) from O1 to the three RE forming one facet of the tetrahedron and a longer one to the forth RE (d^2). Distances for the A-type structure are represented by triangles. The dashed black line indicates the transition volume from the C- to A-type structure, red dotted lines show the equilibrium volumes for both structures.

two O1-RE distances, a shorter one (d^1) from O1 to the three RE forming one facet of the tetrahedron and a longer one to the forth RE (d^2). Therefore, the tetrahedrons are stretched in the z direction and this distortion is slightly more pronounced for the heavier oxides. In particular, for hexagonal Pr_2O_3 the difference between d^1 and d^2 is about 3% whereas for Tm_2O_3 is more than 5% at the transition volume. For all the hexagonal structures there is a tendency for these two distances to become closer to each other under pressure, hence, pressure prompts the tetrahedrons to approach a more ideal configuration. If we look now at the oxygen-RE distances in the C-type phase we will see quite an opposite behavior (Fig. 7). Although the RE tetrahedrons of the cubic phase appear to be distorted as well the application of pressure does not illuminate the distortion but, on the contrary, promotes it. For lighter Re_2O_3 we find that two O-RE distances are very close to each other whereas the third and especially the forth ones are noticeably larger [Fig. 7(a)]. Pressure appears to promote this tendency of oxygen to bind more strongly to the two RE atoms making the RE tetrahedron more and more distorted as volume decreases. Heavier Re_2O_3 show similar behavior, however, in their case all the four O-RE distances in the RE tetrahedron differ from each other. Again we see that extension brings tetrahedrons almost into the ideal configuration whereas pressure makes oxygen atom to increasingly prefer binding to particular RE atoms. We notice that in both A- and C-type structures oxygen tends to form noticeably shorter bonds to the three RE atoms and a longer one to the forth RE of the tetrahedron. Binding to those three RE atoms seems to be important for the relative stability of the structures as there is a correlation between the occurrence of the phase transition and the crossing of these bonding distances for the C- and A-type structures. Figure 7 illustrates this observation for Pr_2O_3 and Tm_2O_3. Above the transition volume the cubic structure offers somewhat larger average distance between the oxygen and the three RE atoms whereas for the volumes below the transition hexagonal structure provides more space for the oxygen atom.

The analysis of the evolution of the tetrahedron configurations shows that in both structures oxygen can prefer lower coordination number of RE atoms than four, explicitly offered by the tetrahedron arrangement. The notably difference, however, is that pressure appears to promote this trend in the C-type structures and works against it in the A-type oxides (Fig. 7). To see the relation these structural patterns might have to the phase stability, we analyze different contributions to the total energy and their pressure dependences. It is often instructive to divide the total energy into two parts: the band energy E_{band} representing the integral over the occupied one-electron states and the sum of the remaining energy terms dominated by the electrostatic energy.[25,26] Let us designate it here as $E_{el.stat}=E_{tot}-E_{band}$. The E_{band} contribution favors more open structures with low coordination numbers whereas $E_{el.stat}$ tends to stabilize high-symmetry close-packed structures. To analyze the importance of these contributions we compare the volume dependences of total energy [Fig. 8(a)] and value $E_{el.stat}/E_{band}$ [Fig. 8(b)] for the two phases. Mind that E_{band} and total energy are negative whereas $E_{el.stat}$ is positive. Therefore, the negative and positive values of $(E_{el.stat}/E_{band})^C-(E_{el.stat}/E_{band})^A$ [Fig. 8(b)]

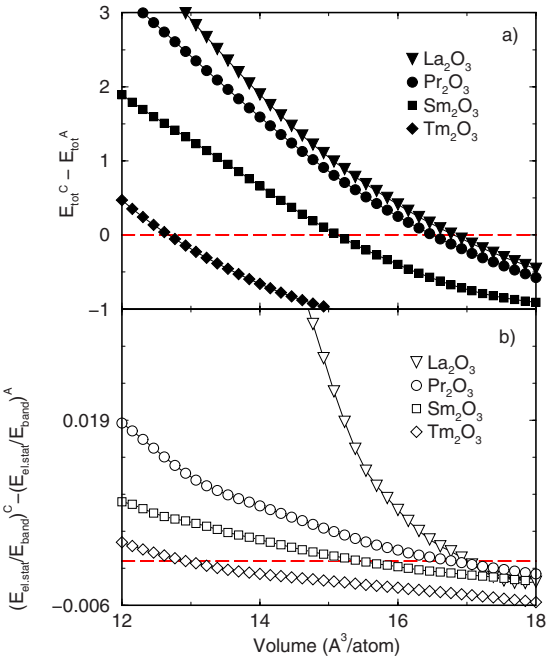

FIG. 8. (Color online) (a) Relative total energy as a function of volume and (b) variation in contributions to the total energy for La_2O_3, Pr_2O_3, Sm_2O_3, and Tm_2O_3 calculated using LDA. All energies are shown with respect to those of A-type oxides: (a) $E_{tot}^C - E_{tot}^A$ and (b) $(E_{el.stat}/E_{band})^C-(E_{el.stat}/E_{band})^A$, where $E_{tot}=E_{band}+E_{el.stat}$.

demonstrate the dominance of the $E_{el.stat}$ term for the C and A phase, respectively. The overall phase stability appears to be determined by the electrostatic contribution to the total energy. Indeed above the transition volume the total energy of the C-type phase has a lower band energy contribution compared to the one of the A-type phase (Fig. 8). On the contrary, the electrostatic contribution is larger for the cubic phase stable at those volumes. Below the transition volume the picture is reversed (Fig. 8). This result correlates well with the structural changes in the two phases described above as the tendency to lower coordination of oxygen is larger for A-type RE_2O_3 than for the C-type oxides above the transition volume and lower below the transition point (Fig. 6).

To gain further insight into the bonding in these oxides we have analyzed their density of states. In agreement with experimental observations all the investigated oxides appear to be insulators exhibiting large gaps between the valence and conduction bands (Fig. 9). The gaps obtained for the C-type structures are systematically lower than those for A-type oxides. GGA and LDA produce virtually the same bandgap for a given volume, however, the GGA equilibrium volumes are larger than the LDA ones. Therefore, the LDA bandgaps calculated for equilibrium volumes (Fig. 9) are larger than the GGA ones that reflects the fact that the gap increases with decreasing volume. This trend holds for all the oxides of the series but the rate of the decrease becomes larger toward the end of the series. It is also more pronounced for the A-type phases. As a result, we observe a growing deviation between the GGA and LDA bandgaps toward heavier oxides, that is, especially noticeable for A-type Er_2O_3, Yb_2O_3, and Lu_2O_3

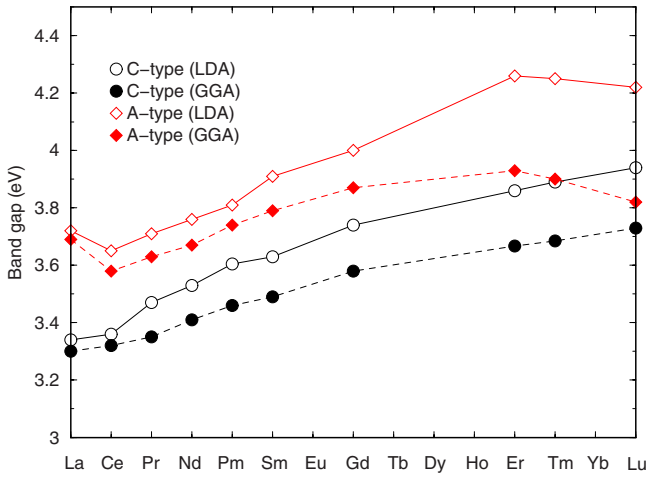

FIG. 9. (Color online) Energy gaps between the conduction and valence bands obtained for the A- and C-type oxides within both LDA and GGA. The bandgaps are shown for the corresponding equilibrium volumes.

(Fig. 9). Notice, however, that in the CSM approach employed here we do not treat the 4*f* orbitals as valence states and, therefore, we miss most important feature of the spectra related to the position of the *f* peak.[11] This serious limitation of the CSM model makes it unsuitable for studying fine electronic effects in these materials. To study the details of electronic spectra one should certainly apply more sophisticated models.[11,17] Nonetheless the obtained partial density of state (PDOS) can give us an additional information about the bonding in the oxides. In Fig. 10 we show PDOS for the A and C phases of Pr_2O_3, as one of the lighter oxides, and Tm_2O_3 representing heavier oxides of the series. In all the cases the valence band is dominated by oxygen *p* states, however, a close comparison of the spectra reveals a substantially larger hybridization between O *p* states and RE *d* and *p* states toward the end of the series. This indicates an increasing contribution of covalent-type bonding in the oxide series.

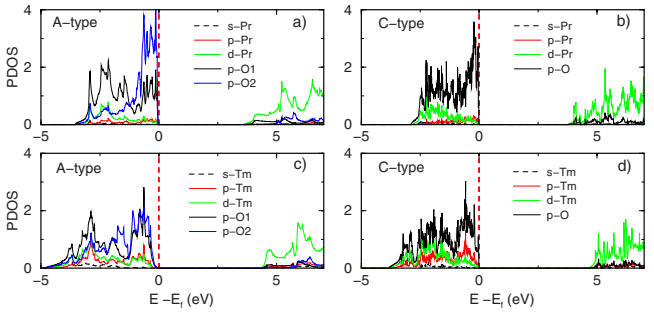

FIG. 10. (Color online) Partial density of states obtained for the A- and C-type phases of [(a) and (b)] Pr_2O_3 and [(c) and (d)] Tm_2O_3 using LDA. Spectra are shown for the corresponding equilibrium volumes.

A substantial contribution of semicore *p*-Tm states to the highest-occupied band is rather surprising and suggests a complex hybridization pattern between the Tm and O states.

IV. CONCLUSION

In conclusion, we have studied the relative stability of the A- and C-type Re_2O_3 oxides under pressure within the core state model. According to both LDA and GGA the pressure of the C- to A-phase transition increases in the series, although, LDA results are in better agreement with available experimental data. Our analysis indicates that the phase stability is determined by the electrostatic contribution to the total energy and related to the relaxation pattern of the structures. Transition pressures are derived from the comparison of the enthalpies of the phases that provides no information about the kinetic aspects of the transition and calls for more experimental and theoretical studies of these systems.

ACKNOWLEDGMENTS

This work has been funded by the Swedish Energy Agency (STEM) and Swedish Research Council (VR). The calculations were performed using the facilities of the Swedish National Infrastructure for Computing (SNIC).

[1] H. Inaba and H. Tagawa, Solid State Ionics **83**, 1 (1996).
[2] A. Trovarelli, *Catalysis by Ceria and Related Materials* (Imperial College, London, 2002).
[3] S. Ohmi, C. Kobayashi, I. Kashiwagi, C. Ohshima, H. Ishiwara, and H. Iwai, J. Electrochem. Soc. **150**, 134 (2003).
[4] L. Eyring, *Handbook on the Physics and Chemistry of Rare Earths 3* (North-Holland, Amsterdam, 1979).
[5] G. Adachi and N. Imanaka, Chem. Rev. (Washington, D.C.) **98**, 1479 (1998).
[6] I. Warshaw and R. Roy, J. Phys. Chem. **65**, 2048 (1961).
[7] H. R. Hoekstra and K. A. Gingerich, Science **146**, 1163 (1964).
[8] N. V. Skorodumova, R. Ahuja, S. I. Simak, I. A. Abrikosov, B. Johansson, and B. I. Lundqvist, Phys. Rev. B **64**, 115108 (2001); D. Anderssons, S. I. Simak, N. V. Skorodumova, I. A. Abrikosov, and B. Johansson, Proc. Natl. Acad. Sci. U.S.A. **103**, 3518 (2006).
[9] N. V. Skorodumova, S. I. Simak, B. I. Lundqvist, I. A. Abrikosov, and B. Johansson, Phys. Rev. Lett. **89**, 166601 (2002).
[10] J. L. F. Da Silva, Phys. Rev. B **76**, 193108 (2007).
[11] L. Petit, A. Svane, Z. Szotek, and W. M. Temmerman, Phys. Rev. B **72**, 205118 (2005).
[12] M. Mikami and S. Nakamura, J. Alloys Compd. **408-412**, 687 (2006).
[13] N. Singh, S. M. Saini, T. Nautiyal, and S. Auluck, J. Appl. Phys. **100**, 083525 (2006).
[14] S. Tanaka, H. Ogasawara, K. Okada, and A. Kotani, J. Phys. Soc. Jpn. **64**, 2225 (1995).
[15] A. Moewes, D. L. Ederer, M. M. Grush, and T. A. Callcott, Phys. Rev. B **59**, 5452 (1999).
[16] N. Hirosaki, S. Ogata, and C. Kocer, J. Alloys Compd. **351**, 31 (2003).
[17] D. A. Andersson, S. I. Simak, B. Johansson, I. A. Abrikosov, and N. V. Skorodumova, Phys. Rev. B **75**, 035109 (2007).
[18] G. Kresse and D. Joubert, Phys. Rev. B **59**, 1758 (1999).

[19] P. E. Blöchl, Phys. Rev. B **50**, 17953 (1994).
[20] G. Kresse and J. Furthmüller, Phys. Rev. B **54**, 11169 (1996)
[21] J. P. Perdew, K. Burke, and M. Ernzerhof, Phys. Rev. Lett. **77**, 3865 (1996).
[22] H. J. Monkhorst and J. D. Pack, Phys. Rev. B **13**, 5188 (1976).
[23] P. E. Blöchl, O. Jepsen, and O. K. Andersen, Phys. Rev. B **49**, 16223 (1994).
[24] F. Birch, Proc. Natl. Acad. Sci. U.S.A. **30**, 244 (1947).
[25] U. Häussermann and S. I. Simak, Phys. Rev. B **64**, 245114 (2001).
[26] N. V. Skorodumova, K. Hermansson, and B. Johansson, Phys. Rev. B **72**, 125414 (2005).